

Electronic Supporting Information for:

The Influence of Polyanion Molecular Weight on Polyelectrolyte Multilayers at Surfaces: Protein Adsorption and Protein-Polysaccharide Complexation/Stripping on Natural Polysaccharide Films on Solid Supports

Natalie L. Benbow^{1,2,3}, Jessie L. Webber^{1,3}, Sam Karpiniec⁴, Marta Krasowska^{1,2,3}, James K.
Ferri⁵ *, and David A. Beattie^{1,2,3} *

¹ *Future Industries Institute, University of South Australia, Mawson Lakes, SA, Australia*

² *Wound Management Innovation Cooperative Research Centre, West End, QLD, Australia*

³ *School of Information Technology and Mathematical Sciences, University of South
Australia, Mawson Lakes Campus, Mawson Lakes, SA 5095*

⁴ *Marinova Pty Ltd, Cambridge, TAS, Australia*

⁵ *Lafayette College, Easton, USA*

* Corresponding Authors: ferrij@lafayette.edu and David.Beattie@unisa.edu.au

Fucoidan Characterisation

Table S.1 Chemical composition of fucoidan polymers^a.

	Carbohydrate (%)							Percent (%)			
	Total ^b	F	X	M	Ga	Gl	R	Sulfate	Cation	Acetyl	Uronic acid
LMWFV	60.1	52.1	3.0	1.5	3.3	0.2	0.1	23.0	6.5	0.0	3.2
FGFV	58.7	44.5	7.1	2.7	3.1	1.3	0.0	28.4	6.0	0.0	3.8

^a Information supplied by Marinova. ^b Total carbohydrate (%) includes: F – fucose, X – xylose, M – mannose, Ga –galactose, Gl - glucose and R – rhamnose.

Table S.2 Molecular weight distribution of fucoidan polymers^a.

Peak Mw	Percentage within Mw ranges (kDa)							
	%> 1600	% 1100-1600	% 200-1100	% 60-200	% 20-60	% 5-20	%< 5	
LMWFV	12.2	1.4	0.3	2.3	6.1	20.2	49.0	20.8
FGFV	117.0	2.4	2.8	34.7	31.4	15.2	4.7	8.8

^a Information supplied by Marinova.

Attenuated Total Reflectance (ATR) FTIR

Polymer Solution Spectra

The ATR FTIR spectra for bulk solutions of chitosan (CS), food grade *Fucus vesiculosus* fucoidan, low molecular weight *Fucus vesiculosus* fucoidan (LMWFV) and bovine serum albumin (BSA) are shown in Figure S.2. The peak assignments for these solution spectra are shown in Table S.3.

All spectra have been processed to remove the background electrolyte signal (using the water bending mode whilst minimising distortion in the 1700 - 1600 cm^{-1} region). It was found that there was a degree of adsorption of the polymers onto the ZnSe crystal, particularly for BSA.¹ This caused non-proportionality between the absorbance of the characteristic peak and concentration. The following process was developed to correct for this. Spectra were collected of the bulk polymer after 15 min pumping at a flow rate of 0.333 mL min^{-1} and then again after a background electrolyte rinse (0.1 M KCl, pH 5 solution, 5 min pumping at a flow rate of 1.000 mL min^{-1}). The spectra collected after each rinse showed the amount of adsorbed polymer on the crystal, this adsorbed amount increased with increasing polymer concentration. The peak area was calculated for the characteristic peaks of both the bulk polymer solution and the spectra of the adsorbed amount left after the electrolyte rinse. The peak area of the adsorbed material was then subtracted from the bulk polymer giving a proportional relationship between absorbance and concentration.

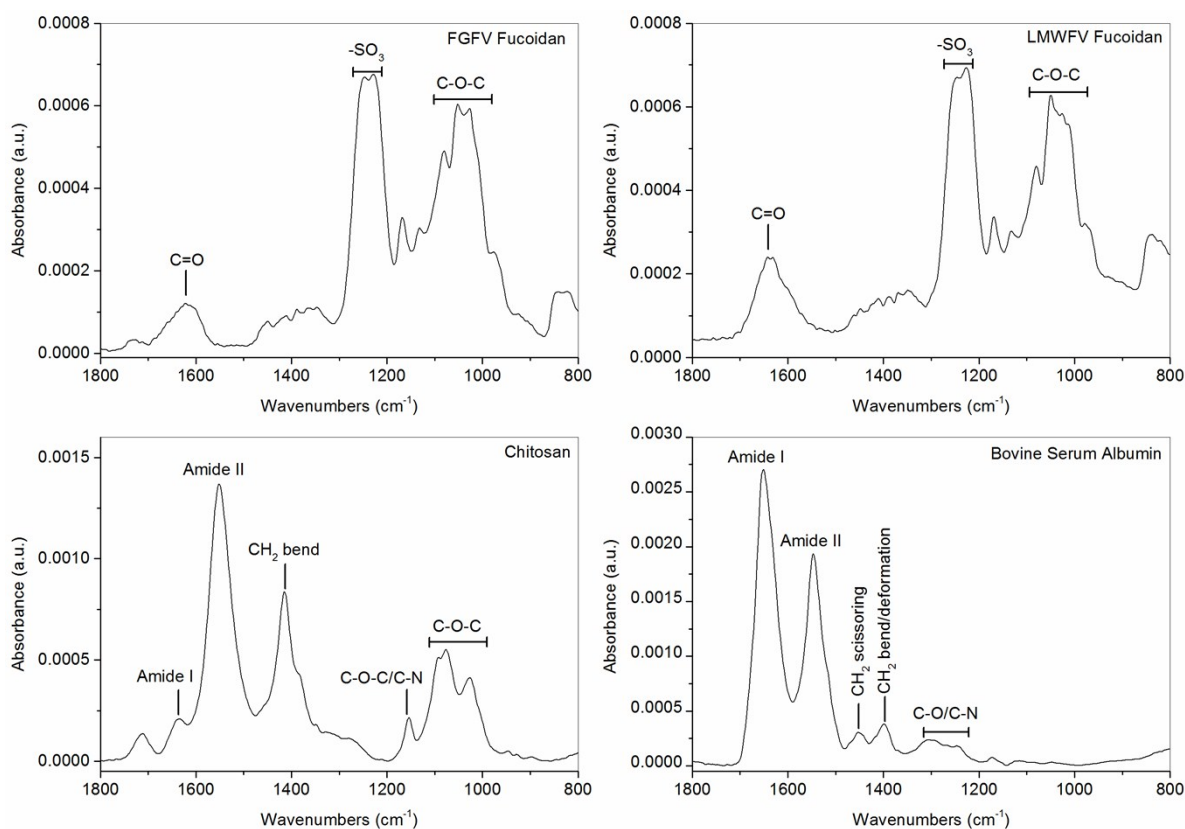


Figure S.1 Major peak assignment for ATR FTIR solution spectra of Low Molecular Weight *Fucus vesiculosus* fucoidan (10,000 ppm in 0.1 M KCl, pH 5), Food Grade *Fucus vesiculosus* fucoidan (10,000 ppm in 0.1 M KCl, pH 5), chitosan (5,000 ppm in 0.1 M KCl, pH 5) and Bovine Serum Albumin (10,000 ppm in 0.1 M KCl, pH 5).

Table S.3 Peak maximum positions and assignments ^{2, 3} for ATR-FTIR spectrum of: 5000 ppm CS, pH 5 in 0.1 M KCl; 10,000 ppm FGFV, pH 5 in 0.1 M KCl; 10,000 ppm LMWFV, pH 5 in 0.1 M KCl; 10,000 ppm BSA, pH 5 in 0.1 M KCl; 7.5-bilayer FGFV/CS polyelectrolyte multilayer with adsorbed BSA; 7.5-bilayer LMWFV/CS polyelectrolyte multilayer with adsorbed BSA.

Peak Assignment	Chitosan Solution	FGFV Solution	LWMFV Solution	BSA Solution
C-O-S		848	848	
Skeletal C-O stretch	1027			
Glycosidic linkage		1052	1048	
Glycosidic linkage	1075	1079	1079	
Glycosidic linkage	1095			
C-O-C/C-N stretch	1153			
C-O-C/C-O stretch		1169	1169	
Sulfonate		1223	1223	
Sulfonate		1249	1249	
CH ₃ deformation	1380			
CH ₂ bending	1415			1399
CH ₂ scissoring		1459	1453	1453
Amide II	1551	1506/1526	1547	1546
C=O		1616 ^a	1636 ^a	
Amide I	1637			1651

^a most likely from uronic acid present in the sample

FTIR Spectra of Individual Layers during PEM Build-up

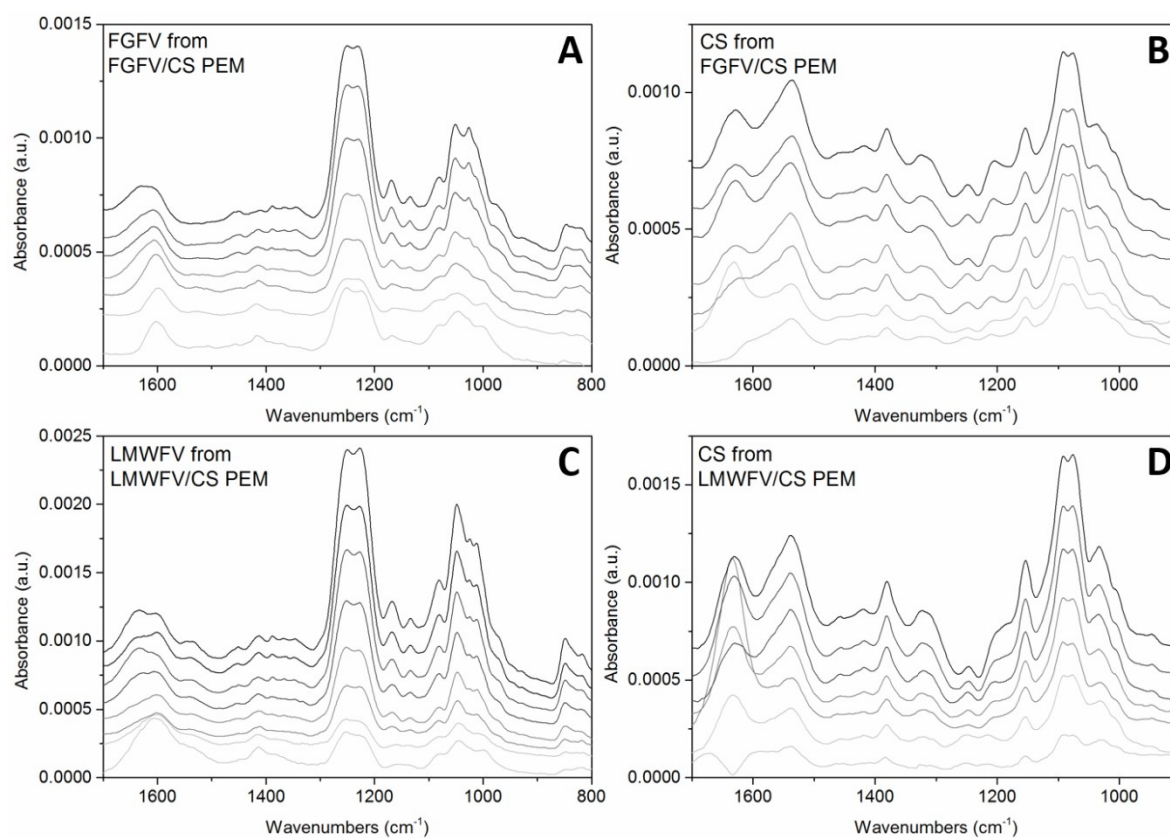


Figure S.2 Individual layer spectra lines (A) FGFV layers and (B) CS layers in the FGFV/CS multilayer; (C) LMWFV layers and (D) CS layers in the LMWFV/CS multilayer.

Quartz Crystal Microbalance with Dissipation monitoring

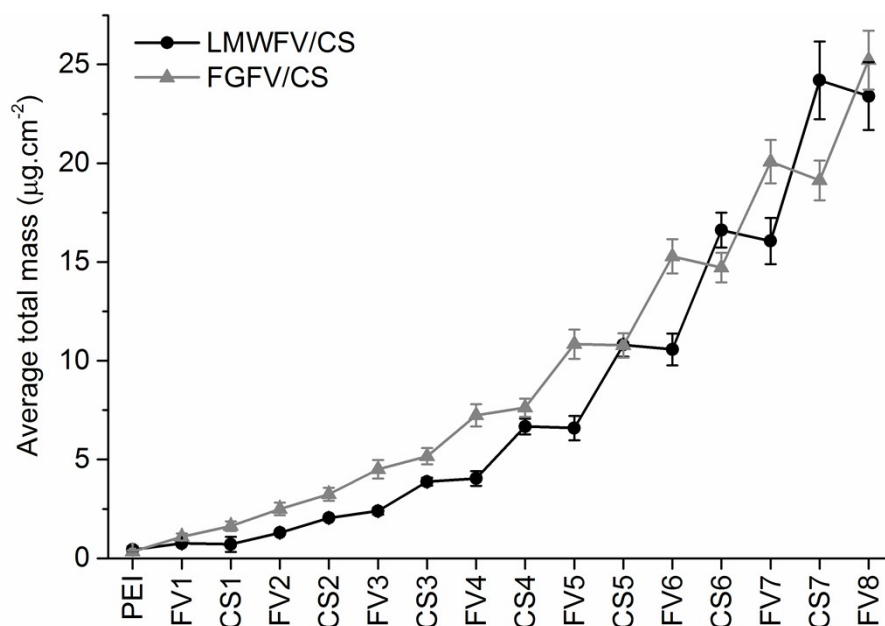


Figure S.3 Average total adsorbed mass by QCM-D of 7.5 bilayers of LMWFV/CS and FGFV/CS multilayers from QCM-D. LMWFV/CS multilayers are indicated by a black line, whilst FGFV/CS multilayers are marked with grey. The average mass is calculated from multiple sensors from two experiments for each multilayer.

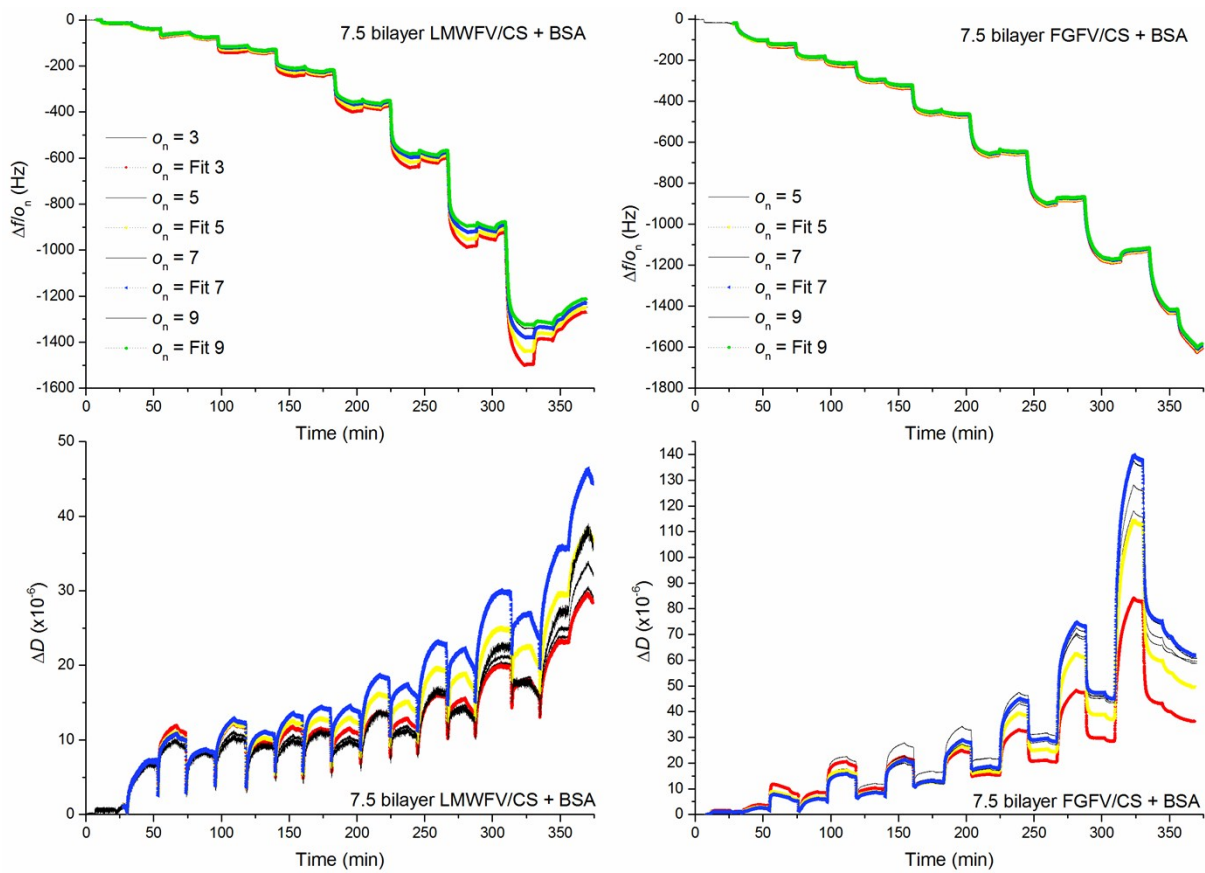


Figure S.4: QCM-D data for the formation of (FGFV/CH)_{7.5} (left) and (LMWFV/CH)_{7.5} (right). Frequency (3rd, 5th, 7th, and 9th overtone) and dissipation (3rd, 5th, 7th, and 9th overtone) are used to perform Voigt fitting for the determination of the viscoelastic properties of the films. Tabulated data from the Voigt fitting is presented in the main manuscript.

Amide I FTIR Peak Deconvolution

The literature for FTIR spectroscopy of BSA display a range of methods for extraction of the relative amounts of amide I components, to ascertain the balance of secondary structures present in a sample.³⁻⁶ The most rigorous method involves the fitting of second derivative spectra to determine relative amounts of the different secondary structures.^{7, 8} However, this method is not universally applicable, as it is often difficult to determine the position of the baseline in such a processed spectra. That being said, second derivative analysis is the best means to determine the actual peak position of the different overlapping components.

We have adopted a hybrid approach that takes into account the presence of an overlapping amide II region (which is split into sub-components, as is the amide I region, albeit not used for determining protein secondary structures), and uses second derivative analysis to underpin the peak deconvolution. Figure S.5 (top panel) contains the full range spectrum (1800 cm^{-1} to 900 cm^{-1}) of a BSA solution, including the peak deconvolution of both amide I and amide II regions. Figure S.5 (middle panel) has a plot of the spectrum and its second derivative in the expanded region between 1750 cm^{-1} and 1450 cm^{-1} , to show the position of the second derivative components, and the corresponding peaks in the spectral deconvolution. The lower panel of the figure highlights the four components of the amide I region that are quantified and discussed in the manuscript.

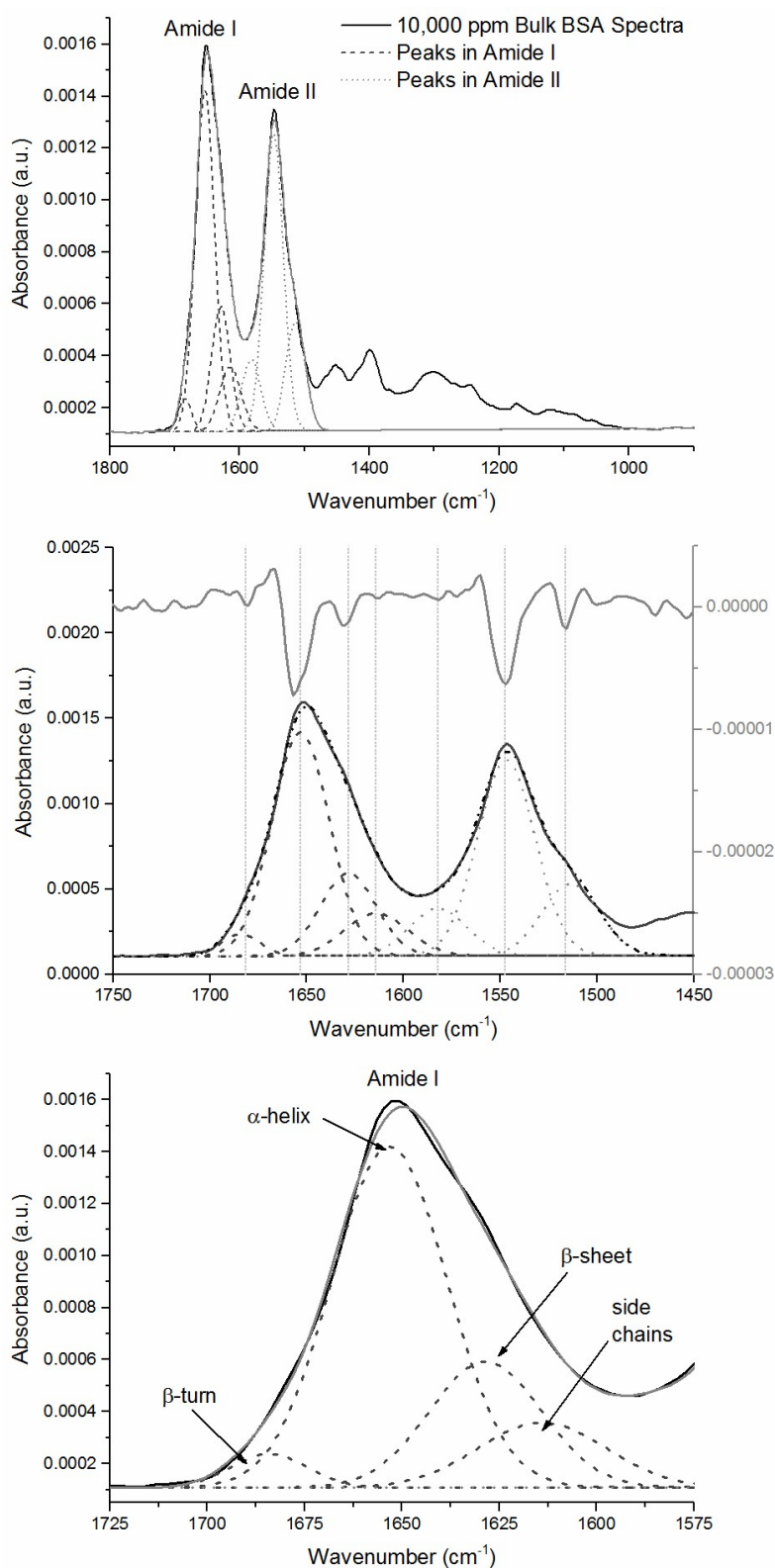


Figure S.5 ATR-FTIR spectra for Bovine Serum Albumin (10,000 ppm in 0.1 M KCl, pH 5); (A) the region between 1800 – 800 cm⁻¹ containing the amide I/II and glycosidic linkage bands showing a flat baseline fitted by incorporating dummy peaks in the amide II band; (B) shows the second derivative and original spectrum aligned to determine peak positions for the amide I/II bands and; (C) amide I band of BSA showing the peak fit of the secondary structure components.³

QCM D-f Plot for Protein Adsorption on a FGFV/CS Multilayer

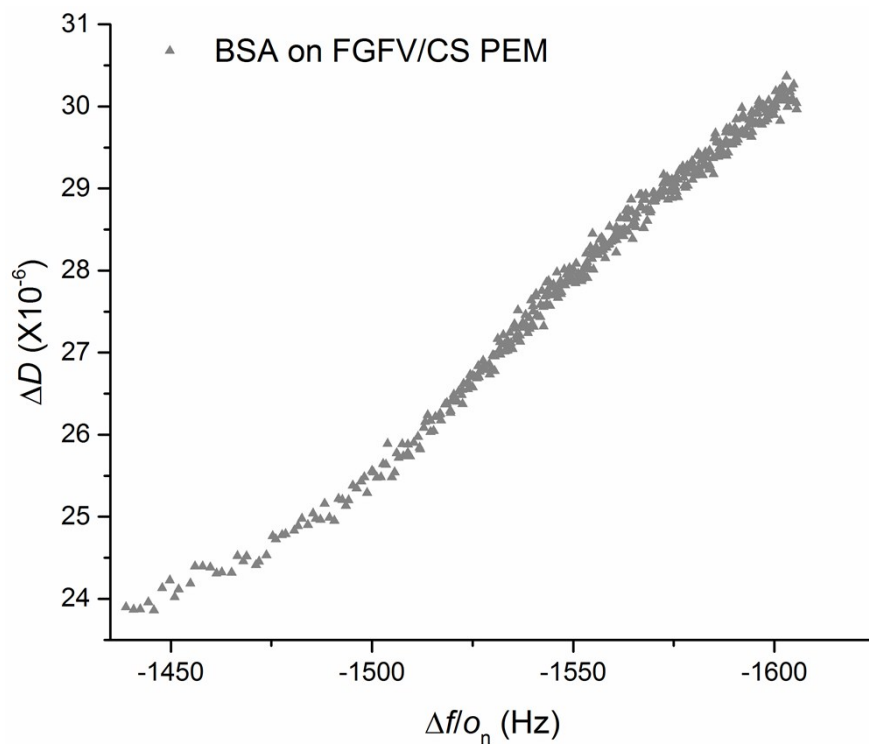


Figure S.6 The ΔD - Δf plot for BSA adsorption onto FGFV/CS multilayer (axes start at measured values for protein adsorption of a representative data set).

UV – Visible Spectroscopy of Protein-Polysaccharide Complexation

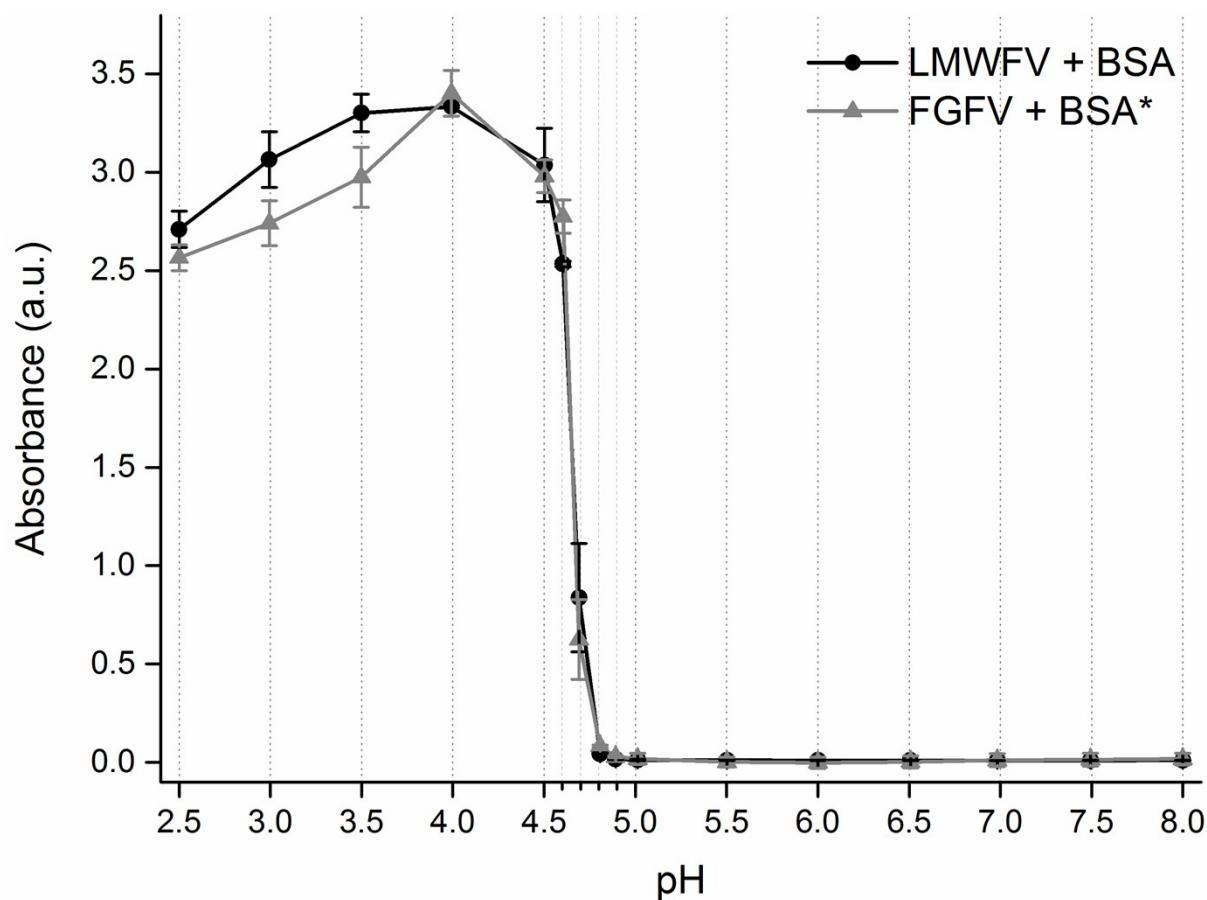


Figure S.7 Solution turbidity by UV-vis spectroscopy (514 nm) for BSA/FGFV and BSA/LMWFV solutions as a function of pH. Using a ratio of 5:1 as specified by Kim *et al.*⁹ but a concentration three times smaller (BSA: 16,675 ppm in 0.1 M KCl and fucoidan: 3,300 ppm in 0.1 M KCl). Note: The FGFV solution is a green/brown colour and so, has an absorbance of approx. 0.3 even when uncomplexed with BSA, however, this has been offset to zero for clarity.

References

1. M. E. Goldberg and A. F. Chaffotte, *Protein Science : A Publication of the Protein Society*, 2005, **14**, 2781-2792.
2. T. T. M. Ho, K. E. Bremmell, M. Krasowska, S. V. MacWilliams, C. J. E. Richard, D. N. Stringer and D. A. Beattie, *Langmuir*, 2015, **31**, 11249-11259.
3. T. Maruyama, S. Katoh, M. Nakajima, H. Nabetani, T. P. Abbott, A. Shono and K. Satoh, *Journal of Membrane Science*, 2001, **192**, 201-207.
4. J.-h. Shi, D.-q. Pan, X.-x. Wang, T.-T. Liu, M. Jiang and Q. Wang, *Journal of Photochemistry and Photobiology B: Biology*, 2016, **162**, 14-23.
5. L. Filali, Y. Brahmi, J. D. Sib, A. Bouhekka, D. Benlakehal, Y. Bouizem, A. Kebab and L. Chahed, *Applied Surface Science*, 2016, **384**, 107-115.
6. R. Lu, W.-W. Li, A. Katzir, Y. Raichlin, H.-Q. Yu and B. Mizaikoff, *Analyst*, 2015, **140**, 765-770.
7. K. K. Chittur, *Biomaterials*, 1998, **19**, 357-369.
8. A. Bouhekka and T. Bürgi, *Applied Surface Science*, 2012, **261**, 369-374.
9. D.-Y. Kim and W.-S. Shin, *Food Hydrocolloids*, 2015, **44**, 471-477.